

**Microstructural Banding and Biaxial Fracture Toughness Tests
in a Specially Heat-Treated Reactor Pressure Vessel Steel**

Randy K. Nanstad
Oak Ridge National Laboratory
P.O. Box 2008
Oak Ridge, TN 37831-6151, USA
865-574-4471 (ph)
865-574-0641 (fax)
nanstadrk@ornl.gov

Mikhail A. Sokolov
Oak Ridge National Laboratory
P.O. Box 2008
Oak Ridge, TN 37831-6151, USA
865-574-4842 (ph)
865-574-0641 (fax)
sokolovm@ornl.gov

Philip J. Maziasz
Oak Ridge National Laboratory
P.O. Box 2008
Oak Ridge, TN 37831-6115,
USA
865-574-5082 (ph)
865-574-7659 (fax)
maziaszpj@ornl.gov

ABSTRACT

The Heavy-Section Steel Technology (HSST) Program at Oak Ridge National Laboratory (ORNL) includes a task to investigate the effects of constraint on the cleavage initiation fracture toughness of reactor pressure vessel (RPV) steels in the lower transition temperature region using relatively large cruciform fracture toughness specimens under varying degrees of biaxial loading. One of the materials used for the project was a plate of A533 grade B steel (HSST Plate 14A) which was specially heat treated to result in a yield strength comparable to that of a radiation-sensitive RPV steel near the end of design life. During the testing phase to characterize the fracture toughness behavior of the plate with uniaxial three-point bend specimens, some relatively low fracture toughness values were observed. Subsequent metallography revealed the presence of varying degrees of dark bands in the microstructure. These observations prompted an investigation of the relationship between the experimentally determined fracture toughness results and the microstructure of the plate steel used for the biaxial-loading effects project, especially with regard to the results obtained from the biaxial test specimens. The

primary issue in the investigation is whether the fracture toughness results obtained from the biaxially loaded specimens were influenced by the steel microstructure in a biased manner; i.e., were the observations regarding effects of biaxial loading on fracture toughness significantly affected by the microstructural segregation in heat treated HSST Plate 14A. A secondary issue is whether segregated microstructures are common in steels used for RPV construction and if the current procedures for evaluating fracture toughness of RPV steels adequately account for such microstructures. Various metallurgical tools, including metallography, microhardness testing, scanning electron fractography, electron microprobe analysis, and analytical electron microscopy were used to characterize the nature of the bands and evaluate the potential effects on the fracture toughness results.

Keywords: fracture toughness, pressure vessel, banding, metallography, fractography, segregation

INTRODUCTION

The Heavy-Section Steel Technology (HSST) Program at Oak Ridge National Laboratory (ORNL) includes a task to investigate the effects of constraint on the cleavage initiation fracture toughness of reactor pressure vessel (RPV) steels in the lower transition temperature region using relatively large cruciform fracture toughness specimens under varying degrees of biaxial loading. One of the materials used for the project was a plate of A533 grade B steel which was specially heat treated to result in a yield strength comparable to that of a radiation-sensitive RPV steel near the end of design life. During the testing phase to characterize the fracture toughness behavior of the plate with uniaxial three-point bend specimens, some relatively low fracture toughness values were observed. Subsequent metallography revealed the presence of varying degrees of dark bands in the microstructure. These observations prompted an investigation of the relationship between the experimentally determined fracture toughness results and the microstructure of the plate steel used for the biaxial-loading effects project, especially with regard to the results obtained from the biaxial test specimens. The primary issue in the investigation is whether the fracture toughness results obtained from the biaxially loaded specimens were influenced by the steel microstructure in a biased manner; i.e., were the observations regarding effects of biaxial loading on fracture toughness significantly affected by the microstructural segregation in heat treated HSST Plate 14A. A secondary issue is whether segregated microstructures are common in steels used for RPV construction and if the current procedures for evaluating fracture toughness of RPV steels adequately account for such microstructures. A detailed description of the biaxial-loading effects project is contained in Ref. [1a], and a complete description of the work described in this paper is presented in Ref. [1b]. Various metallurgical tools, including metallography, microhardness testing, scanning electron fractography, electron microprobe analysis, and analytical electron microscopy were used to characterize the nature of the bands and evaluate the potential effects on the fracture toughness results.

MATERIAL DESCRIPTION

Identification, Chemical Composition, and Heat Treatment

HSST Plate 14 was the original source of material for the cruciform specimens and for the characterization material. In its as-received

condition, Plate 14 conformed to the American Society of Testing and Materials (ASTM) "Specification For Pressure Vessel Plates, Alloy Steel, Quenched And Tempered, Manganese-Molybdenum and Manganese-Molybdenum-Nickel," and met the requirements for A533 grade B class 1. The plate was produced by Marrel Freres. The records show that the plate was originally austenitized at 1607°F (875°C), quenched (presumably in water), and tempered at 1275°F (691°C). Unfortunately, the documents do not provide the holding times during the austenitization or temper treatments. The records of tensile tests on the as-received plate indicate a yield strength of about 402 MPa (58.3 ksi). The chemical composition of Plate 14 is provided in Table 1. Since the objective was to use a material with elevated yield strength, Plate 14 was selected because it has a relatively high carbon content (0.22 wt %), making it somewhat more responsive to heat treatment than the other materials available to the project at the time. A segment of Plate 14, 254 × 122 × 23 cm thick (100 × 48 × 9-1/8 in.), was sent to Lenape Forge in West Chester, Pennsylvania, for the special heat treatment. A thermal buffer was welded around the entire plate segment and the plate was austenitized at 1650°F (899°C) for 12 h, quenched in water, and tempered in air at 825°F (441°C) for 5 h. A test block was removed from one corner of the plate and used to make verification test specimens. The goal was to achieve a room temperature yield strength approximately in the range 620 to 690 MPa (90 to 100 ksi). The verification tests indicated a yield strength of 614 MPa (89 ksi) and the heat treated plate (designated HSST Plate 14A) was accepted by the HSST Program.

Mechanical Properties

Tensile, Charpy V-notch (CVN) impact, and drop-weight tests were performed to characterize the mechanical properties for use in normalizing the fracture toughness test results and for comparison with prototypic RPV steels. The tensile results are summarized in Table 2. The CVN results showed a substantial increase in the transition temperature and were comparable with data from an irradiated submerged-arc weld metal evaluated in the Heavy-Section Steel Irradiation (HSSI) Program [1c]. The drop-weight nil-ductility transition (NDT) temperature and the reference temperature, RT_{NDT} , were found to be 40°C (104°F). Thus, the yield strength and ductile-brittle transition temperatures are both substantially elevated relative to prototypic RPV steel plates in the unirradiated condition.

Table 1. Chemical composition of HSST Plate 14

C	Mn	P	S	Si	Mo	Ni	Cu	Cr
0.22	1.44	0.005	0.003	0.20	0.56	0.62	0.05	0.06

Table 2. Summary of tensile properties of heat-treated HSST Plate 14A

Tensile properties	Temperature	
	-30°C (-22°F)	-5°C (23°F)
Proportional limit [MPa (ksi)]	534 (77.5)	511 (74.2)
0.2% offset yield strength [MPa (ksi)]	669 (97.0)	653 (94.7)
Ultimate strength [MPa (ksi)]	848 (123)	828 (120.2)

FRACTURE TOUGHNESS RESULTS

To characterize the fracture toughness of the plate material, 0.5T compact specimens [0.5TC(T)] were tested at ORNL over the temperature range expected for conduct of the biaxial tests. These specimens were machined from four different blocks at different locations within the heat treated plate to sample potential variability within the parent plate. The specimen orientation was L-S, the same as that for the biaxial specimens. Following

specimen size adjustment according to ASTM E-1921, the T_0 value was determined to be -37°C (-35°F). Subsequently, additional 0.5T specimens were machined from five different blocks of the heat treated plate and the overall T_0 value was determined to be -51°C (-60°F). Fig. 1 shows the detailed test results.

Material was also provided to the Naval Surface Warfare Center (NSWC) in Carderock, Maryland, for the conduct of uniaxial 1T three-point bend

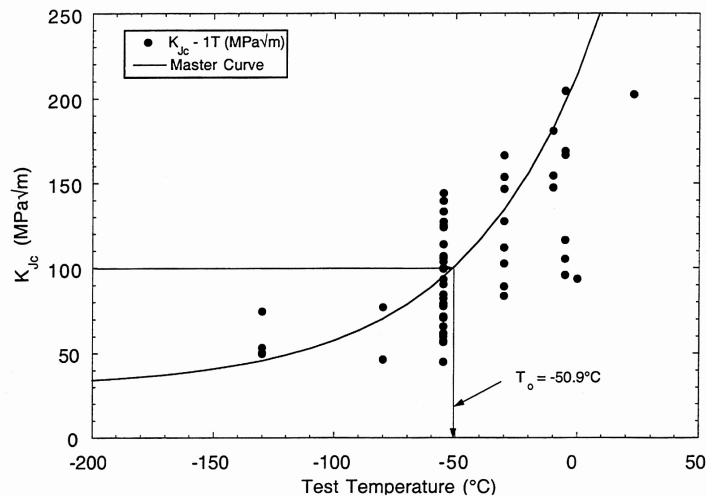
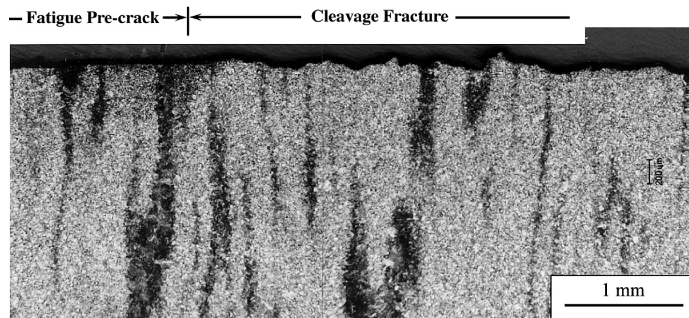
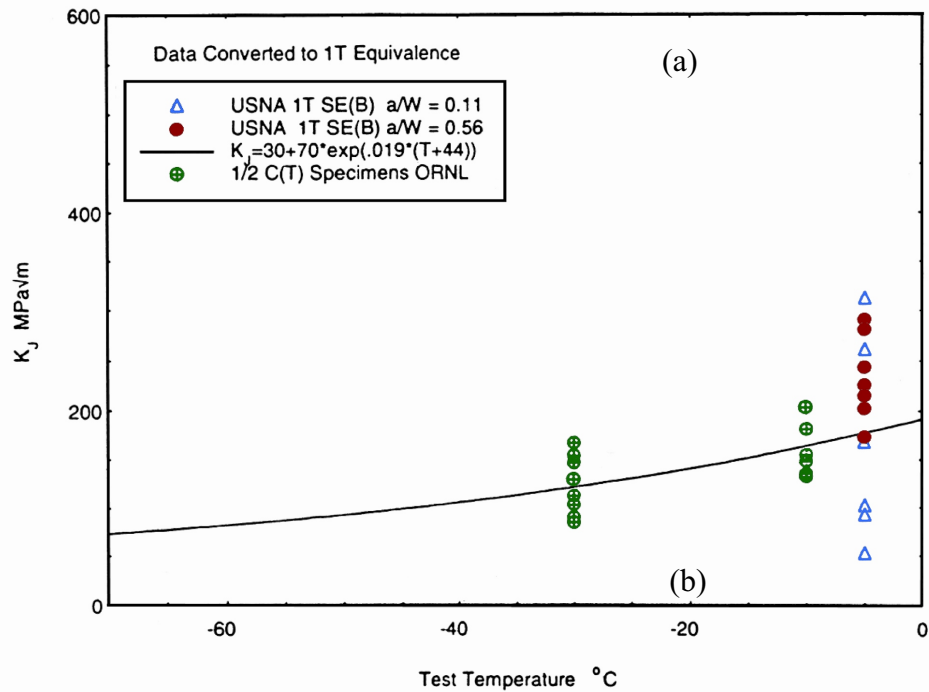


Figure 1. Fracture toughness data from 0.5T compact specimens of heat-treated HSST Plate 14A showing Master Curve and data. All data are adjusted to 1T size in this figure.

[1TSE(B)] tests [the tests were conducted for NSWC by the United States Naval Academy (USNA)]. Eight shallow-flaw and seven deep-flaw specimens were tested at -5°C . The results of those tests are shown in Fig. 2 [Ref. 2]. Shallow-flaw specimen P14S7 was tested at -5°C and gave the lowest fracture toughness ($51\text{MPa}\sqrt{\text{m}}$) at that temperature and was significantly lower than the next lowest result ($90.7\text{MPa}\sqrt{\text{m}}$). Furthermore, a number of the shallow-flaw specimens exhibited lower fracture toughness than the deep-flaw specimens tested at the same temperature, an unexpected result. Micrographs of that specimen and others were prepared by NSWC and provided

to ORNL by NSWC; they showed varying degrees of dark bands which were assumed to be due to microstructural banding. Fractography was also performed by NSWC and indicated that the fatigue crack fronts were in regions of banding in some cases. The micrograph for specimen P14S7, shown in Fig. 2, exhibited very dark bands and that observation provided the postulate that the banded regions may be the cause of the low fracture toughness results. At the same temperature, another NSWC tested shallow flaw specimen (P14S4) also exhibited apparent banding, albeit not so heavy as P14S7, and gave the highest fracture toughness ($311\text{MPa}\sqrt{\text{m}}$) in the scatter band.



Specimen P14S7 (USNA)

Figure 2. Plot of fracture toughness data from 1T three-point bend specimens of heat-treated HSST Plate 14A, and composite micrograph of 1T bend specimen P14S7 (data and micrograph provided by USNA and NSWC).

Figures 3(a) and (b) shows a schematic drawing with dimensions and a photograph, respectively, of the intermediate size cruciform biaxial specimens with nominal thickness of about 100 mm [1]. The fracture toughness results from these tests will be

fractography and metallography. A fracture surface of each specimen was examined in a Philips XL-30 field emission gun scanning electron microscope (SEM) to characterize the fracture mode and morphology, and to identify and locate the cleavage initiation site (cleavage origin). Measurements of

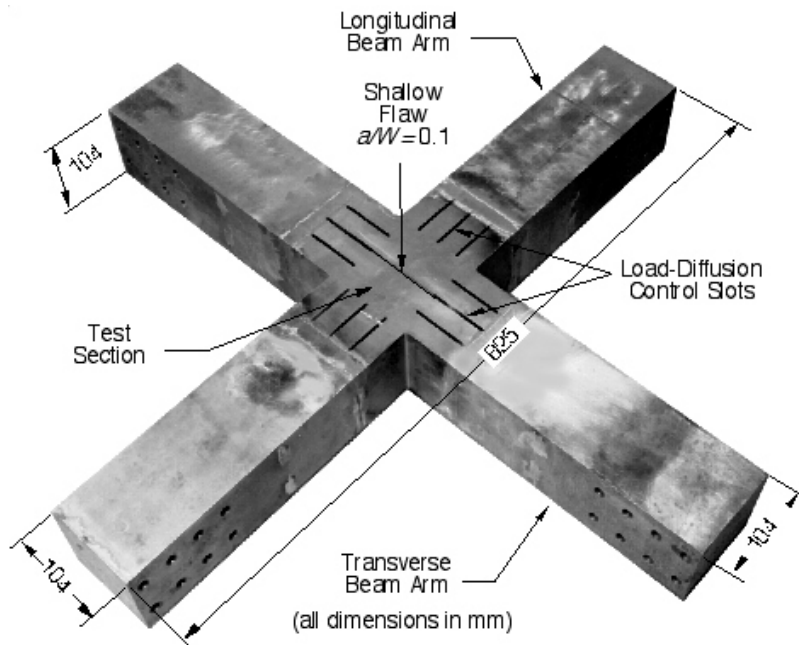


Figure 3. Geometry of the cruciform shallow-flaw biaxial fracture toughness test specimen (type A): (a) schematic drawing showing various features of the specimen, and (b) photograph of a typical specimen prior to testing.

discussed in a later section.

MICROSTRUCTURAL AND FRACTOGRAPHIC EXAMINATIONS

Procedures

Some of the fracture toughness specimens and all of the biaxial test specimens were examined by

the fatigue crack length, any precleavage ductile crack extension, and distance from the crack tip to the cleavage origin were performed on the SEM. The fracture surface was then sectioned perpendicular to the surface near the cleavage origin and submitted for metallography. Figure 4 is a schematic representation of the process. Grinding and polishing were followed by a number of trials with various etchants and etchant combinations; 4 grams picric acid with 100 ml ethanol and immersion for about 3 min. was chosen as the best

one to reveal the nature of the banded regions in the microstructure. Micrographs were then made at various magnifications from the fatigue precrack region to beyond the site of the cleavage origin. The micrographs were then assembled in

wide range of microhardness in the microstructure and a significantly higher hardness in a darkly etching banded region of the microstructure, 418 μH , compared with the matrix hardness, 252 μH . Figure 5(a) shows an intermediate hardness of 304

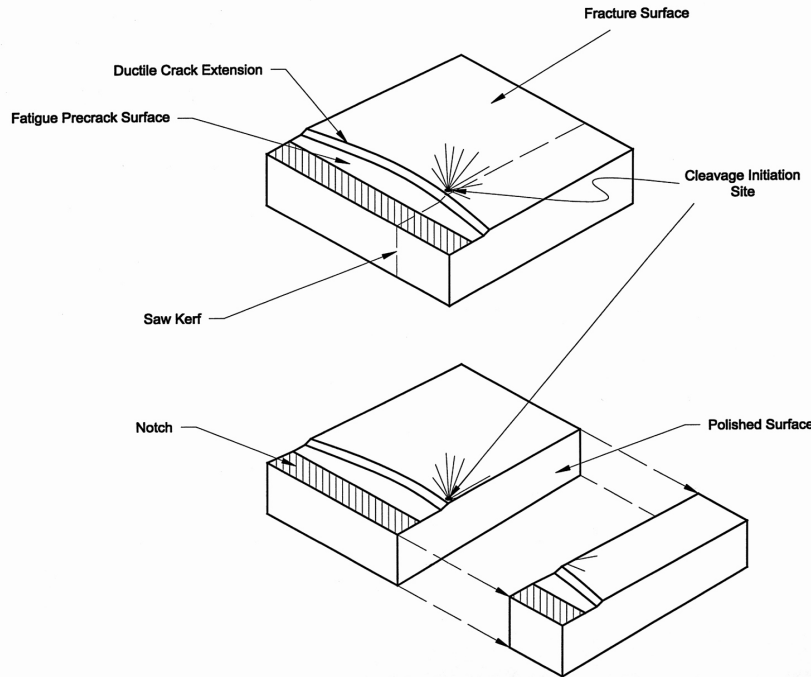


Figure 4. Schematic diagram showing procedure for preparing metallographic sample to examine relationship of fracture surface features and microstructures in heat-treated HSST Plate 14A.

composite fashion to provide a continuous view of the microstructure through the region of interest. Microanalysis and transmission electron microscopy were also performed to characterize the nature of the banding; the specific procedures will be discussed in a later section.

Microhardness Traverse

A full thickness slice of Plate 14A was prepared with a fine-ground finish and microhardness tests were conducted across the thickness at intervals of about 6 mm. The results showed substantial scatter but no gradient from near surface to center of the plate. Moreover, metallography revealed no apparent macrosegregation or microsegregation in that portion of Plate 14A.

Fractographic and Metallographic Examinations of Characterization Test Specimens

Figure 5 presents the results of microhardness tests on 0.5TC(T) specimen JP-06 and shows a

μH in a lighter etching banded region. the microstructure outside of the banded regions is representative of an as-quenched microstructure because the temper treatment given this material was very slight. The microstructure contains some proeutectoid ferrite with what are likely martensite-austenite constituents and carbides in a banded microstructure, although transmission electron microscopy is needed to verify that supposition. In the segregated regions, the microstructure is finer with less proeutectoid ferrite and appears to have a more martensitic appearance, which also corresponds to the much higher hardness compared with the nonsegregated regions.

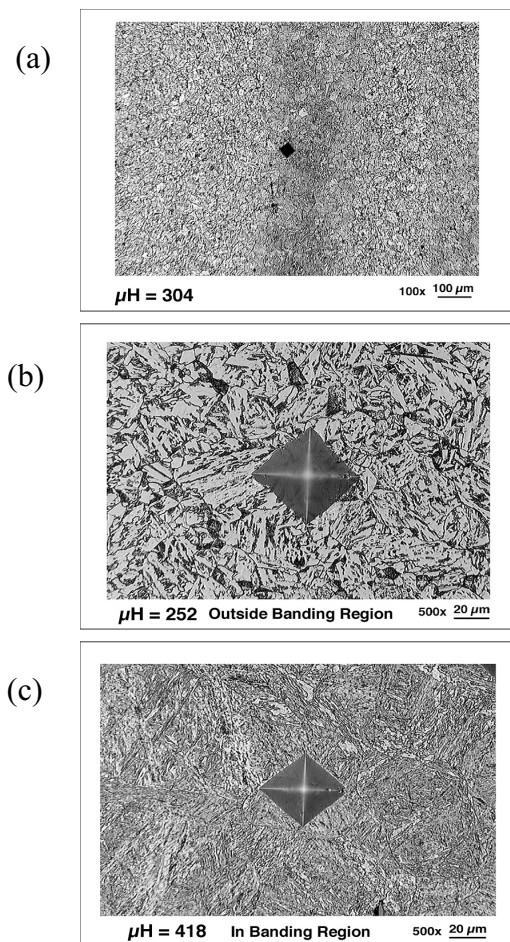


Figure 5. Microhardness of various regions in microstructure of 0.5T compact specimen JP-06 from heat-treated HSST Plate 14A, showing microhardness comparisons in (a) light-etching band, (b) matrix outside bands, and (c) dark-etching band.

Scanning electron fractography of 0.5TC(T) specimens JP-01 and JP-06 confirmed the observations of prefracture stable tearing and that the fracture mode in each case was cleavage. Fractographic examinations of the 1T bend specimens by NSWC revealed similar observations [1]. For specimen JP-06, Fig. 6(a) provides a low magnification fractograph that shows the fatigue precrack, precleavage ductile crack extension, and the region of the cleavage origin, while Fig. 6(b) provides a view of the cleavage origin at higher magnification. Similar fractographs for specimen JP-01, showed that specimen exhibited no precleavage ductile crack extension. Note on Fig. 6(a) that the crack extended through a relatively heavy band and that the cleavage origin does not appear to be associated with a region of banding. For JP-01, however, similar micrographs show that there is a heavy band just in front of the crack tip and the cleavage origin appears to be close to that band.

A composite micrograph for specimen P14S7 (tested by USNA) was provided by NSWC and was shown earlier in Fig. 2; the etchant used by NSWC was 2% nital. NSWC also provided a portion of that specimen to ORNL so it could be examined, re-polished, and etched in the same manner as the ORNL specimens. The SEM examination was not successful in identifying a single cleavage origin, and concluded that multiple origins existed along the crack front. Because the fracture toughness of specimen P14S7 was so low, 51.5 MPa \sqrt{m} , there was no ductile tearing and the cleavage origin is undoubtedly just slightly ahead of the fatigue crack. Such an observation is common for specimens which fail at relatively low fracture toughness. Although the relationships between the microstructural features and the fatigue crack front are somewhat different in the two micrographs, both views result in the existence of bands near the crack front and associated with the cleavage origin, which is presumed to be just slightly ahead of the crack front, at least at the specific location in the specimen thickness. Another view at a different position through the thickness of the specimen, however, revealed no areas of banding in the region of the crack front, demonstrating the varying relationship between the crack tip and the microstructural features..

More recent tests with 1T three-point bend shallow flaw specimens have been conducted at ORNL for additional characterization. Two of those specimens exhibited interesting behavior relative to the microstructural effects under discussion. SEM fractographs and a composite micrograph for

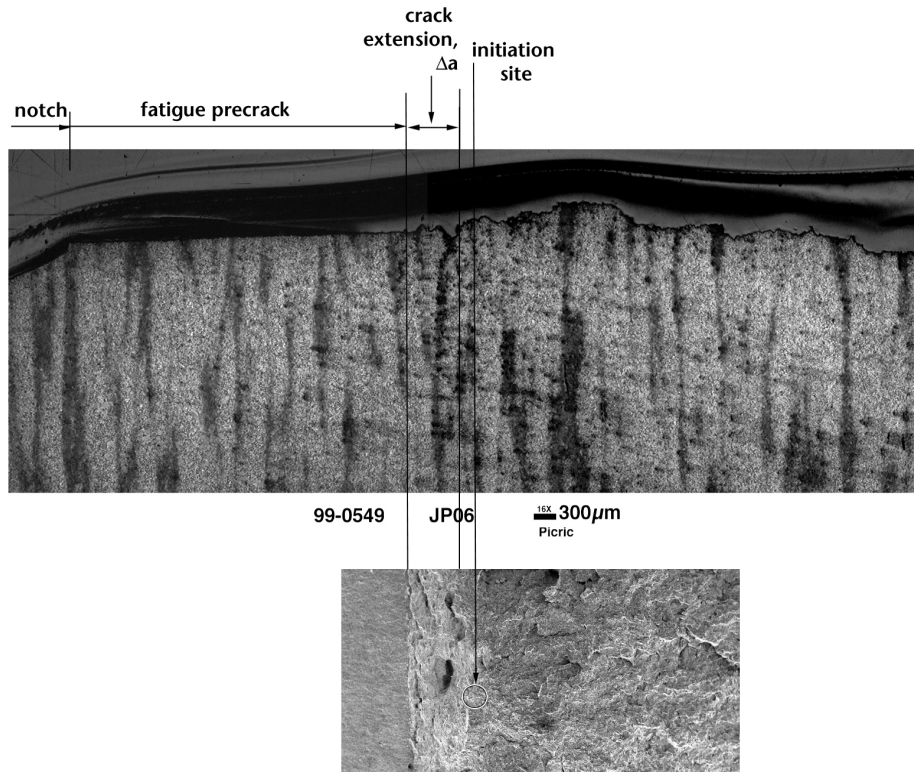


Figure 6. Composite micrographic pan (top) and scanning electron fractograph (bottom) of 0.5T compact specimen JP-06 from heat-treated HSST Plate 14A, showing relationship between fracture surface features and the microstructure in the vicinity of the cleavage initiation site.

specimen PBS-16, tested at -20°C , showed that the fatigue precrack was pinned at one particular point along the crack front which inhibited further crack growth at that particular point. The composite micrograph showed that the pinned portion corresponded to a rather large area of segregation where the cleavage initiation is located. More detailed views of the pinned area showed indications of intergranular fracture in the cavity formed by pull-out of material during the fracture process. This specimen failed at a K_{Jc} value of $63.6 \text{ MPa}\sqrt{\text{m}}$, a value which is rather low within the database for this material. Another specimen, PBS-12, was also tested at -20°C and failed at a K_{Jc} of $120.5 \text{ MPa}\sqrt{\text{m}}$. In this case, however, the fatigue precrack propagated through a similarly heavy area of segregation. Additionally, a heavy band was located just in front of the crack front, but the cleavage origin was located well ahead of the band. Furthermore, there were elements of intergranular fracture in the region of the band

through which the fatigue crack propagated.

Fractographic and Metallographic Examinations of Biaxial Test Specimens

SEM and metallographic examinations were performed for 13 biaxial test specimens of HSST Plate 14A. Composite micrographs were prepared for all those specimens and are provided in Ref. [1c]. Table 3 provides a summary of the fracture toughness test results and the SEM measurements. The specimens are listed generally in order of increasing test temperature, biaxial loading ratio, and fracture toughness. At the location through the specimen thickness where the

Table 3. Summary of relationship between fracture toughness and microstructure for HSST Plate 14A

Specimen ID	Biaxial Ratio	Test Temp °C	K_{Jc} MPa√m	Fatigue Crack	Δa mm	$\Delta a + X$ mm	X mm	0.75X' mm	2X' mm	Bands Between Crack Tip & Origin	Origin in Band	Bands Within 0.75X'	Bands Within 2X'
P12B	0	-30	88.0	2.73	0	0.28	0.28	0.053	0.142	Y	Y	Y	Y
P14B	0.6	-30	70.3	1.60	0	Multi	NM	0.034	0.091	N	N	N	YWea
P4A	1	-30	141.2	3.02	0	0.163	0.163	0.138	0.367	Y	Y	Y	Y
P13A	0	-5	184.2		0	0.282	0.282	0.234	0.624	Y	N	Y	Y
P9A	0	-5	381.8		1.410	1.570	0.160	1.005	2.681	N	N	Y	Y
P18A	0	-5	280.5	2.76	0.430	0.630	0.200	0.543	1.447	NWea	Y	Y	Y
P17B	1	-5	129.5	3.20	0	0.250	0.250	0.115	0.308	N	N	N	N
P6B	1	-5	162.3	3.77	0	0.328 or 0.193	0.328 or 0.193	0.182 ^a	0.484 ^a	Y	Y	Y	Y
										Y	YClos	Y	Y
P5B	1	-5	316.1	2.64	0.83	1.130	0.300	0.689	1.838	YWea	N	YWea	Y
P4B	1	5	167.5	2.65	0	0.300	0.300	0.194	0.516	N	N	N	N
P6A	0.6	5	195.2	3.73	0.132	0.448	0.316	0.263	0.701	N	N	N	N
P11A	0.6	16	238.2	2.77	0	0.250	0.250	0.391	1.043	N	N	N	N
P11B	1	16	325.5	3.43	1.26	1.43	0.170	0.731	1.949	Y	N	Y	Y
JP-06	0	-5	264.4		0.75	0.92	0.170	0.482	1.286	N	N	N	NWea
JP-01	0	-5	121.5		0	0.27	0.270	0.102	0.271	Y	YClos	Y	Y
P14S7	0	-5	51.5		0	Multi	NM	0.018	0.049	Y N	Ywea N	Y N	Y N
PBS12	0	-20	120.5					0.100	0.267	Y	N	Y	Y
PBS16	0	-20	63.6					0.028	0.074	Y	Y	Y	Y

cleavage origin was located, the table provides the length of the fatigue crack, the ductile crack extension, and the distance from the crack front at the time of fracture to the cleavage origin.

It is not especially clear how to judge the relationship between the fracture toughness and the local microstructure in the region of the crack front in any particular specimen. A simple qualitative judgement is quite observer dependent. To provide a more consistent basis, a semiquantitative procedure was developed. The last two columns in Table 3 are calculated distances based on the relationship,

$$X' = X_c / (J_c / S_Y) \quad (1)$$

where X' is the normalized distance versus cleavage fracture toughness, K_{Jc} , from a cleavage initiation site database [Ref. 1], X_c is the distance from the cleavage origin to the crack front at the time of fracture, J_c is the value of the J-integral at the time of fracture, and S_Y is the material yield strength. About 80% of the data are located at values of X' of about 2.0 or less [3]. Another plot, also from Ref. 3, which demonstrates the sensitivity to biaxiality for Q-stress based on the maximum principal stress ahead of the crack, shows the peak stress location occurs at about $0.75X'$. Thus, the columns labeled $2X'$ and $0.75X'$ in Table 3 reflect the corresponding values of X_c . Finally, the last four columns of Table 3 provide the results of the micrograph examinations relative to the relationship or lack thereof between the crack front, the cleavage origin, the peak stress location, and that volume of material ahead of the crack front within

which one would expect to see about 80% of the cleavage initiation sites. Relative to the stress distribution, the value of $2X'$ is well beyond the peak stress location. The observations are given as yes or no (Y or N), although some cases include comments such as “weak” (i.e., a lightly etching band) or “close” (i.e., not exactly in the band but very close to it).

The following example illustrates the process. Figure 7 for specimen P11B shows that the crack front coincides with a band in this specimen, but the cleavage origin is not associated with a band. Thus, Table 3 indicates a “Y” and a “N” for the first two columns related to existence of bands. Since the distance $0.75X$ is greater than the distance for X , then a band does exist within the distance $0.75X$ as well as within the distance $2X$, and the last two columns indicate “Y.” Figure 8 is shown for specimen P4A because it demonstrates contrast with that of figure 7 for P11B in that the cleavage origin is associated with a band. Both specimens (biaxial ratios of 1) had bands between the crack tip and origin, but gave K_{Jc} results of 141.2 and 325.5 Mpa√m, respectively.

Microanalysis Examinations

To better understand the nature of the segregation features observable in the optical microstructure of the polished and etched samples from the biaxial specimens, two additional analyses were conducted: (1) X-ray microcompositional analysis of the matrix and segregation regions was performed on a JOEL 733 Superprobe instrument; and (2) qualitative analysis of the carbides on a carbon-film

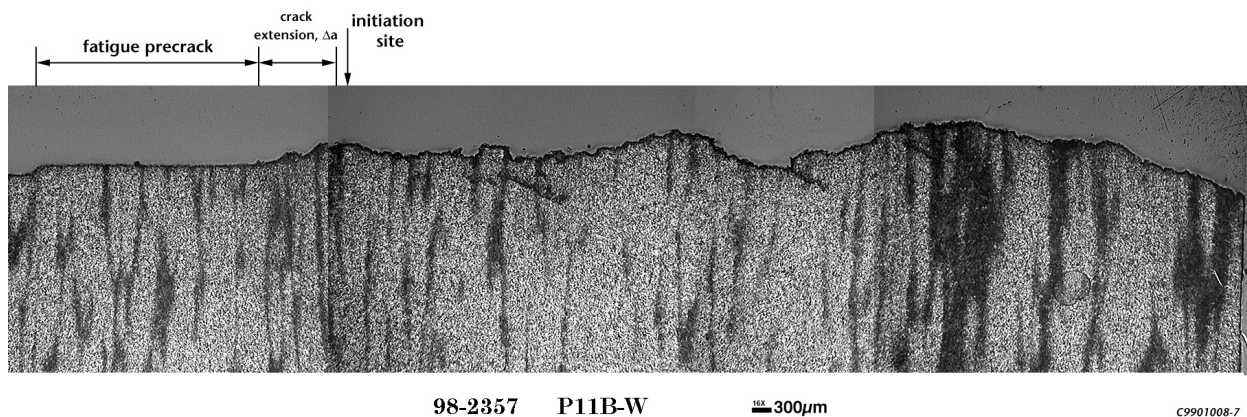
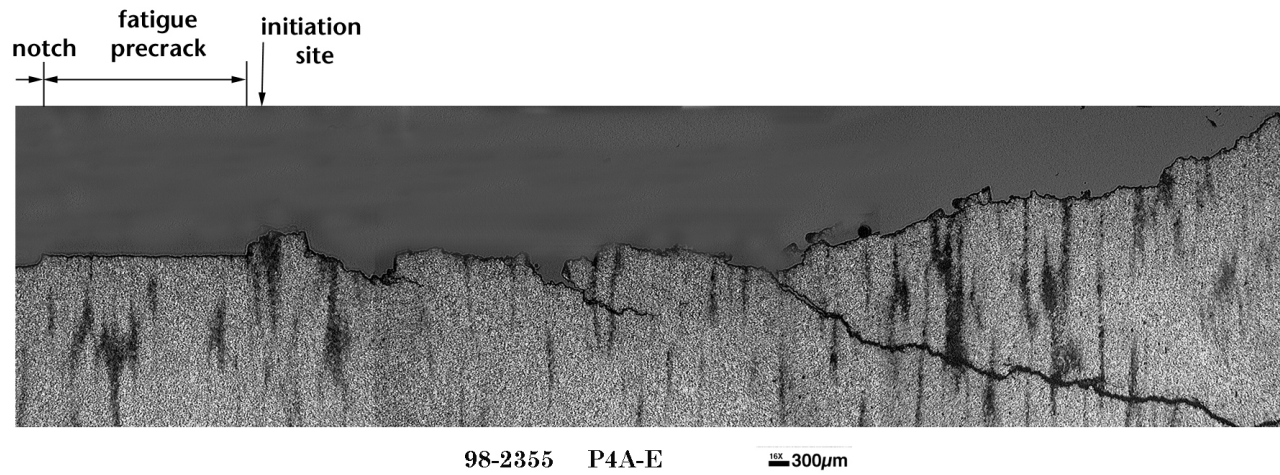
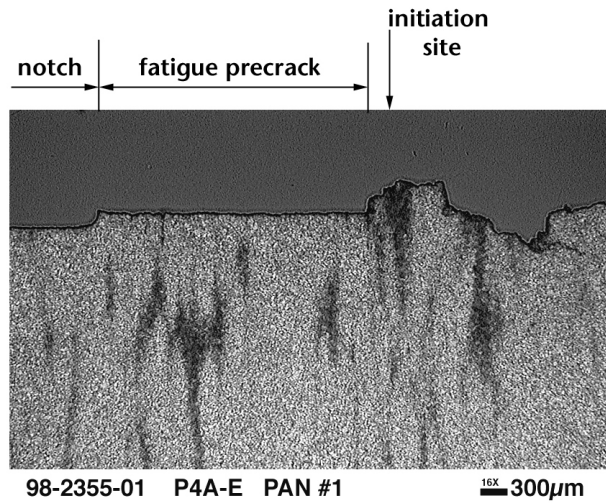


Figure 7. Composite micrographic pan of shallow-flaw biaxial specimen P11B of heat-treated HSST Plate 14A tested with a biaxial ratio of 1.0 at 16°C.



11



C9901008-5

Figure 8. Composite micrographic pan of shallow-flaw biaxial specimen P4A of heat-treated HSST Plate 14A tested with a biaxial ratio of 1 at -30°C.

extraction-replica was performed using a Philips CM200 field-emission gun (FEG, 200 KV) analytical electron microscope (AEM). As stated earlier, the term “banding” typically refers to the inhomogeneity of alternating ferrite and pearlite microstructures on the order of a grain size and does result from microsegregation of alloying elements. In heat-treated HSST Plate 14, the alternating microstructural regions are not ferrite and pearlite

as in carbon steels, but we will refer to the phenomenon in this steel as banding in any case because it is descriptive of the microstructural observations. Figure 9 shows one example with specimen JP-06. Quantitative wavelength- and energy-dispersive X-ray spectroscopy microprobe scans across the segregated regions show that they are much richer in molybdenum and manganese relative to the surrounding ferritic

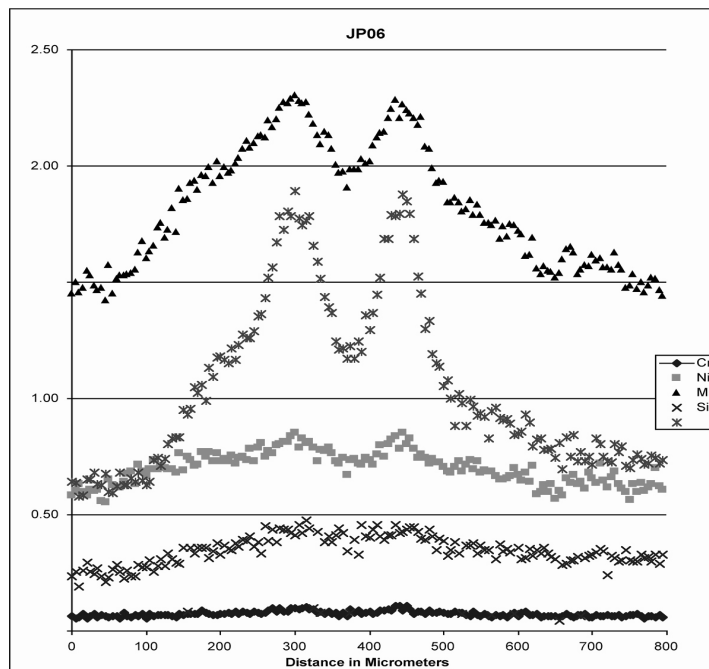
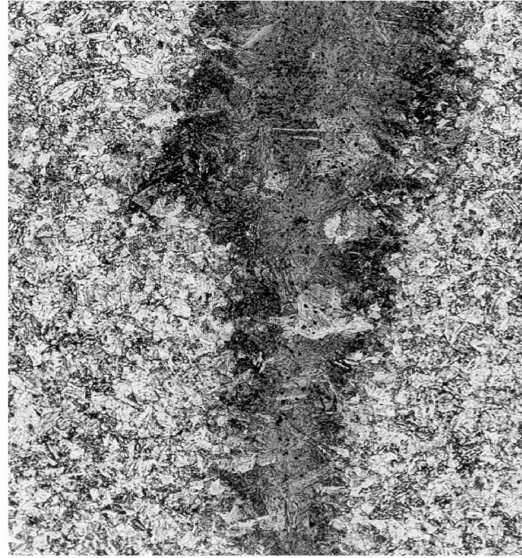


Figure 9. X-ray compositional microanalysis results across large area of segregation in 0.5T compact specimen JP-06 from heat-treated HSST Plate 14A.

matrix. Substantial enrichment in nickel and silicon are also evident, but chromium and copper do not appear to be segregates. Similar analyses show the degree of segregation is lower in the lighter etching regions than in the darker etching regions. These elements are substitutional alloying elements that are rejected into the liquid phase of the steel during the initial solidification and casting process, and can be retained interdendritically as well as in the center of an ingot. The subsequent mechanical processing (e.g., hot rolling) and heat treating procedures will affect the degree of microsegregation and macrosegregation which results. However, the spacial resolution of the electron beam and corresponding X-ray excited volume (at 20 KV) do not allow the composition of individual carbide particles to be measured. This analysis alone cannot determine whether the carbides are rich in molybdenum and/or manganese or whether the matrix is enriched in those elements.

To provide a more in-depth answer, carbon-film extraction replicas were prepared from the banded regions of specimen JP-01 and analyzed on a state-of-the-art AEM with a super-fine electron probe (FEG, 1-2 nm) and windowless X-ray energy dispersive spectroscopy (XEDS) detector. AEM analysis of many individual carbide particles, and then broad-beam analyses of clusters of hundreds or thousands of carbides shows that all are Fe_3C iron-carbides with traces of manganese and no detectable molybdenum.

The interpretation of this analysis suggests that molybdenum and manganese are inhomogeneities that are caused during the initial casting and solidification, and then retained during the subsequent wrought processing and heat-treatments. Those elements may cause the austenite-to-ferrite transformation to be more sluggish than regions without those solutes, hence making them higher in carbon than the surrounding matrix and more heavily carbide-precipitated after tempering. This is one possibility that would relate the heavier carbide precipitation to regions rich in those solutes, and also correlate with such regions being harder than the surrounding matrix. One critical test of the above suggestion would be if higher temperature solution-annealing and homogenization prior to tempering reduced or eliminated such "carbide-banding" features, and made the carbide distribution more uniform.

DISCUSSION

Some Observations of Banding in the Literature

As stated by Thompson and Howell [4], "Banding is a term used to describe a microstructure consisting of alternate layers of proeutectoid ferrite and (frequently) pearlite, as opposed to a random distribution of these microstructural constituents." Various postulates have been offered over the years to explain the cause of banding. References 5-8 provide detailed discussions of banding and are summarized in ref. 1b. In heat-treated HSST Plate 14A, of course, the nature of the banding is not classical in that sense because the microstructure is not composed of proeutectoid ferrite and pearlite. Because of the very low tempering conditions (441°C for 5 h), the microstructure is closer to that of an as-quenched microstructure which, in this steel, consists generally of bainite, martensite, and proeutectoid ferrite. Although the fabrication details for the plate in the original condition are not known, it was re-austenitized for 12 h for the biaxial effects study, which should be sufficient time for elemental re-resolution. Again, a more detailed discussion is presented in ref. 1b.

As stated earlier, a secondary issue of this investigation is whether segregated microstructures are common in steels used for RPV construction and if the current procedures for evaluating fracture toughness of RPV steels adequately account for such microstructures. In a separate HSST Program study to evaluate J-integral resistance curve behavior, six plates of A302 grade B (modified) and one plate of A533 grade B class 1 steel were tested [10]. The apparent degrees of segregation are variable, but it was evident that all seven steels exhibit some amount of segregation. The A533 grade B class 1 plate exhibited the darkest etching microstructure of the eight steels and was selected for microanalysis and comparison with the heat treated Plate 14A samples. The analyses showed that significant and similar segregation exists in that material. Microstructural studies conducted for the HSST Program at the University of Tennessee in 1970 [11], observed similar microstructural segregation in HSST Plate 01, a plate of the same size and heat treatment as HSST Plate 02, both of which were used extensively in establishment of the fracture toughness guidelines currently in use in the American Society of Mechanical Engineers (ASME) Boiler and Pressure Vessel Code. *It is noteworthy that Plate 02, in particular, provided the fracture toughness data which dominated the construction of the lower-bound fracture toughness curves referenced to RT_{NDT} .* Pugh, Edwards, and Druce [12] provided an example of similar banding in a 150-mm-thick plate of A533 grade B class 1 steel. Although an extensive review has not been

conducted in this study, it appears that banding-type segregation in RPV steels is not uncommon.

A more detailed review of refs. 13-21 regarding the effects of banding type segregation on mechanical properties is discussed in ref. 1b.

In a study of HY-80 steel heat treated to produce a mixed microstructure of tough martensite and brittle bainite, Hagiwara and Knott [22] observed that the K_{Ic} values showed particularly large scatter with a bimodal distribution. They reported that fractography showed the upper branch of the fracture toughness distribution corresponded to the presence of the tough phase at a calculated critical distance ahead of the crack tip, while the lower branch was associated with the brittle phase in that position. This observation is shown schematically in Fig. 10. Knott [23] further stated "The general principles involved would appear to have application to a wide variety of mixed microstructures, including banded plate and weld metals."

Thus, the concept which emerges is that a mixed microstructure of relatively brittle and ductile microstructures will increase the overall scatter in toughness to include lower values caused by interaction of the crack tip stress-strain field with the

brittle phase. Although this concept seems conceptually plausible, development of a quantitative model would require considerable research, including experimental, analytical, and modeling studies. For example, in the case of the banding-type of segregation observed in the heat treated Plate 14A, it was pointed out earlier that the segregation varies in hardness. Assuming a general correlation of higher yield strength and lower toughness with increased hardness in a given material, a wide variety of strength differences will exist on the microstructural scale. An additional complication will accrue because of the varying physical sizes of the segregated regions.

Apparent Effects of Segregation on Heat-Treated HSST Plate 14A

Simply from a qualitative perspective, the fracture toughness results discussed earlier for 1T bend bars would lead one to the conclusion that the heavily segregated microstructure of heat-treated HSST Plate 14A resulted in some unusually low cleavage fracture toughness values. However, as stated earlier, the primary issue in the current investigation is whether the fracture toughness results obtained from the biaxially loaded specimens were influenced by the steel microstructure in a biased manner. The results presented in Table 3 regarding the relationship between the specimen crack front, the cleavage origin, and a specified volume of material ahead of the crack front are used for such an evaluation in the following manner. In Fig. 11, the data points corresponding to the biaxial specimens tested at -5°C have been annotated with the results contained in the first two columns of Table 3 for the crack front/microstructure relationship (i.e., the "bands between crack tip and origin" and the "origin in band"). The fracture toughness results indicate the lack of a biaxial effect at a temperature near the lower shelf (Figure not shown), as well as a measurable biaxial effect in the transition region (Fig 11). The crack front/microstructure observations appear to be mixed in the sense that both low and high values of fracture toughness are associated to some degree with the segregated microstructure. Relative to the overall results, Fig. 12 shows a similar plot of all the cruciform specimen

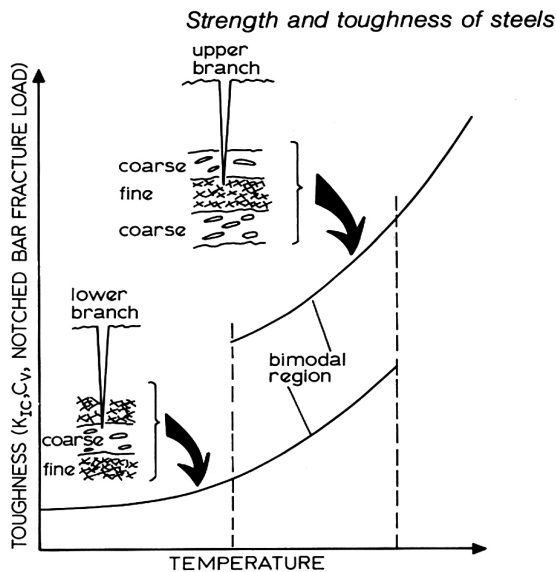


Figure 10. Schematic diagram of "bimodal" toughness behavior and suggested explanation in terms of coarse (brittle) and fine (tough) phases and their location with respect to the crack tip (Ref. 22).

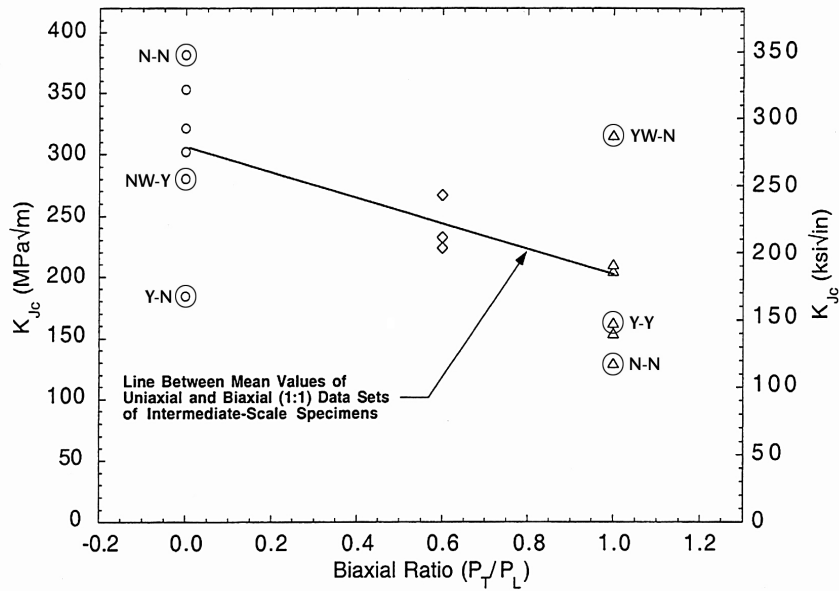


Figure 11. The effect of biaxial load ratio on fracture toughness determined for heat-treated HSST Plate 14A tested at -5°C (23°F). The Y and N annotations relate to the apparent association or lack thereof between the crack front and cleavage origin, respectively (see Table 3).

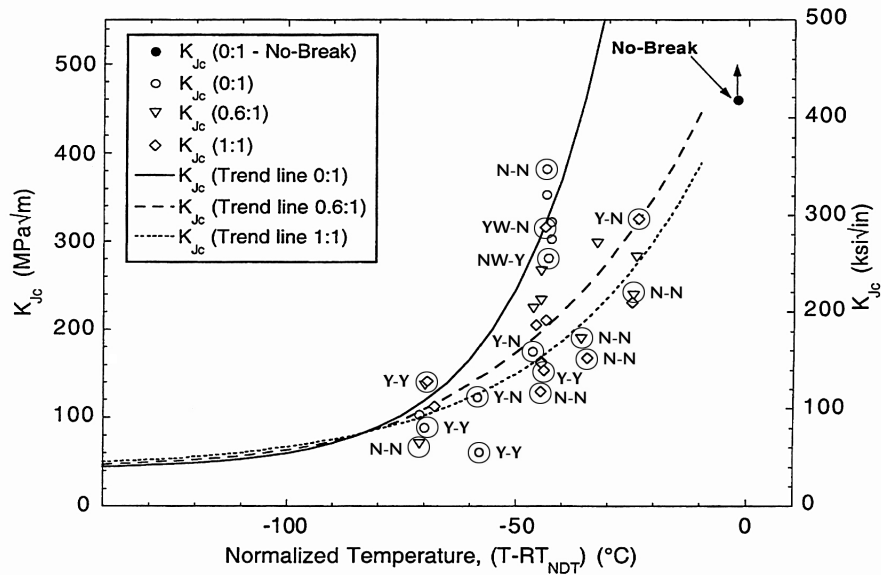


Figure 12. A summary of all heat-treated HSST Plate 14A cruciform data presented as a function of normalized ($T - RT_{NDT}$) test temperature. Trend curves fitted to data provide a visual interpretation of relationship between biaxial loading and temperature. The Y and N annotations relate to the apparent association or lack thereof between the crack front and cleavage origin, respectively (see Table 3).

data with annotations as in the previous figures. Again, the crack front/microstructure observations appear to be mixed at both low and high values of fracture toughness. There are a number of relatively low fracture toughness results which do not appear to be associated with regions of microstructural segregation. Moreover, the mixed results occur for all three biaxial load ratios. Additionally, a number of the results with (N, N) annotations also do not have bands between the crack front and the peak stress location ($0.75X'$) nor the volume ahead of the crack at a distance of $2X'$. Thus, this evaluation points to an unbiased effect of the segregated microstructure on the observations regarding biaxial effects on fracture toughness.

With regard to the secondary objective, that of whether the current procedures for evaluating fracture toughness of RPV steels adequately account for such microstructures, it is apparent that banding-type microstructural segregation in commercial RPV steels is very common. This includes at least one of the steels used for development of the fracture toughness and crack-arrest toughness databases currently used for structural integrity evaluations. Although the information regarding effects of such segregation on cleavage fracture toughness is rather sparse, the indications are that such banding-type segregation leads to a rather modest increase in the ductile-brittle transition temperature. Of course, the effect of the segregation would undoubtedly be dependent on the "degree" of segregation, e.g., as in the "lightly etching" vs "darkly etching" microstructures presented earlier.

Finally, it is noted that heat-treated HSST Plate 14A was heat-treated to produce mechanical properties which are not representative of A533 grade B class 1 plate in the as-received condition. This material had a significantly higher yield strength and ductile-brittle transition temperature than required by the material specification. This does not invalidate the results from a fracture mechanics perspective, but it is an important distinction relative to the steels used for RPV construction. The conclusion of this evaluation is that the overall observations do not give cause for concern regarding application of the current databases to RPV integrity. As a note of caution, however, it is also noted that insufficient testing of an individual steel from a statistical standpoint could lead to non-conservative results if that steel is characterized by substantial microstructural segregation.

SUMMARY AND CONCLUSIONS

Fracture toughness characterization specimens and relatively large biaxially-loaded cruciform specimens have been examined fractographically and metallographically to evaluate the effects of banding-type microstructural segregation on the biaxial fracture toughness results. The primary issue is whether the fracture toughness results obtained from the biaxially loaded specimens were influenced by the steel microstructure in a biased manner; i.e., were the observations regarding effects of biaxial loading on fracture toughness significantly affected by the microstructural segregation in heat treated HSST Plate 14A. A secondary issue is whether segregated microstructures are common in steels used for RPV construction and if the current procedures for evaluating fracture toughness of RPV steels adequately account for such microstructures. The main conclusions are as follows:

1. The heavily segregated microstructure of specially heat-treated HSST Plate 14A did appear to result in some unusually low cleavage fracture toughness values.
2. Evaluation of the crack front/microstructure relationships for the biaxial test specimens points to an unbiased effect of the segregated microstructure on the observations regarding biaxial effects on fracture toughness.
3. Given the demonstrated common observations of banding-type microstructural segregation in commercial RPV steels, the overall observations do not give cause for concern regarding application of the current ASME Code fracture toughness databases to RPV integrity.
4. It is noted that insufficient testing of an individual steel from a statistical standpoint could lead to non-conservative results if that steel is characterized by substantial microstructural segregation.

ACKNOWLEDGMENTS

This research is sponsored by the Office of Nuclear Regulatory Research, U.S. Nuclear Regulatory Commission, under Interagency Agreement DOE 1886-N011-9B with the U.S. Department of Energy under Contract No. DE-AC05-00OR22725 with U.T.-Battelle, LLC.

REFERENCES

- 1a. B.R. Bass, W. J. McAfee, P. T. Williams, T. L. Dickson, D. E. McCabe, C. E. Pugh, and W. E. Pennell, *Research Results Supporting Enhanced Fracture Analysis Methods for Nuclear Reactor Pressure Vessels*, NUREG/CR-6657, draft report, October 1999.
- 1b. Nanstad, R.K., Sokolov, M.A., and Maziasz, P.J., "Microstructural Banding and Biaxial Fracture Toughness Tests in a Specially Heat-Treated Reactor Pressure Vessel Steel," *ORNL/NRC/LTR-00/01*, Oak Ridge National laboratory, April, 2000.
- 1c. Nanstad, R.K., McCabe, D.E., Menke, B.H., Iskander, S.K., and Haggag, F.M., "Effects of Radiation on Kic Curves for High Copper Welds," *Effects of Radiation on Materials: 14th International Symposium (Volume ii)*, ASTM STP 1046, N.H. Packan, R.E. Stoller, and A.S. Kumar, Eds., American Society for Testing and Materials, Philadelphia, 1990, pp. 214-233.
2. J. A. Joyce, R. L. Tregoning, and X. J. Zhang, "Application of Master Curve Technology to Biaxial and Shallow Crack Fracture Data for A 533B Steels," pp. 177-203 in *Effects of Radiation on Materials: 19th International Symposium*, ASTM STP 1366, M. L. Hamilton, A. S. Kumar, S. T. Rosinski, and M. L. Grossbeck, Eds., American Society for Testing and Materials, West Conshohocken, Pa., March 2000.
3. P. T. Williams, B. R. Bass, and W. J. McAfee, "Shallow Flaws under Biaxial Loading Conditions, Part II: Application of a Weibull Stress Analysis of the Cruciform Bend Specimen Using a Hydrostatic Stress Criterion," pp. 75-85 in *Advances in Life Prediction Methodology*, PVP Vol. 391, R. Mohan, Ed., presented at the 1999 ASME Pressure Vessels and Piping Conference, Boston, August 1-5, 1999.
4. S. W. Thompson and P. R. Howell, "Factors Influencing Ferrite/Pearlite Banding and Origin of Large Pearlite Nodules in a Hypoeutectoid Plate Steel," *Materials Science and Technology*, Vol. 8, September 1992.
5. C. F. Jatczak, D. J. Firardi, and E. S. Rowland: *Trans. ASM*, 1956, 48, 279-303.
6. P. G. Bastien, *J. Iron Steel Inst.*, 1957, 187, 281-291.
7. J. S. Kirkaldy, J. von Destinon-forstmann, and R. J. Brigham: *Can Metall. Q.*, 1962, 1, 59-81.
8. J. A. Eckert, P. R. Howell, and S. W. Thompson, "Banding and the Nature of Large, Irregular Pearlite Nodules in a Hot-Rolled Low-Alloy Plate Steel: A Second Report," *Journal of Materials Science* 28(16): 4412-4420 (August 15, 1993).
9. R. Pelli, P. Nenonen, M. Kemppainen, and K. Torronen, *Reactor Pressure Vessel Steels ASME SA533B and SA508 Cl. 2, Microstructural Investigations*, Research Report 219, Technical Research Centre of Finland, Espoo, September 1983.
10. D. E. McCabe, E. T. Mannes Schmidt, and R. L. Swain, *Ductile Fracture Toughness of Modified A302 Grade B Plate Materials*, NUREG/CR-6426, Vol. 2 (ORNL-6892/V2), February 1997.
11. J. R. Hester, Jr., "Correlation of Microstructure with Mechanical Properties for HSST Program Plate 01," M. S. Thesis, The University of Tennessee, March 1970.
12. S. F. Pugh, B. C. Edwards, and S. G. Druce, "Problems Involved in the Specification of the Chemical Composition of an LWR Pressure Vessel Steel." pp. 33-68 in *Trends in Reactor Pressure Vessel and Circuit Development*, R. W. Nichols, Ed., Applied Science Publishers, London, 1980.
13. R. G. Hoagland, "Investigations of Fracture Toughness of ASTM A 302, Grade B, Steel with the DCB Specimens," pp. 108-118 in *Heavy-Section Steel Technology Program Semiannual Progress Report for Period Ending February 29, 1968*, ORNL-4315, October 1968.
14. R. A. Grange, "Effect of Microstructural Banding in Steel," *Metallurgical Transactions*, 2, 417-426, February 1971.
15. W. A. Spitzig, "Effect of Sulfide Inclusion Morphology and Pearlite Banding on Anisotropy of Mechanical Properties in Normalized C-Mn Steels," *Metallurgical*

Transactions A, 14A, 271-283,
February 1983.

16. P. Shanmugam and S. D. Pathak, "Some Studies on the Impact Behavior of Banded Microalloyed Steel," *Engineering Fracture Mechanics*, 53(6): 991-1005 (April 1996).
17. A. Ray, S. K. Paul, and S. Jha, "Effect of Inclusions and Microstructural Characteristics on the Mechanical Properties and Fracture Behavior of a High-Strength Low-Alloy Steel," *Journal of Materials Engineering and Performance*, 4, 679-688 (1995).
18. A. Sakir Bor, "Effect of Pearlite Banding on Mechanical Properties of Hot-Rolled Steel Plates," *ISIJ International*, 31(12), 1445-1446, 1991.
19. Standard Practice for Assessing the Degree of Banding or Orientation of Microstructures, E 1268-94, *Annual Book of ASTM Standards*, American Society for Testing and Materials, West Conshohocken, Pa., 1994.
20. H. K. D. H. Bhadeshia, *Bainite in Steels: Transformations, Microstructure, and Properties*, Institute of Metals, London, 1992.
21. P. Bowen, S. G. Druce, and J. F. Knott, *Acta Metallurgica* 34: 1121-1131 (1986).
22. Y. Hagiwara and J. F. Knott, pp. 707 in *Fifth International Congress on Fracture, Cannes*, D. Francois et al., Eds., Pergamon, 1981.
23. J. F. Knott, "Strength and Toughness of Steels," pp. 181-198 in *Proceedings of the International Conference on Advances in the Physical Metallurgy and Application of Steels*, The Metals Society, London, 1982.